INTERNATIONAL JOURNAL OF REFRIGERATION 57 (2015) 229–238

Available online at www.sciencedirect.com

ScienceDirect

journal homepage: www.elsevier.com/locate/ijrefrig

Real-time thermal load calculation by automatic estimation of convection coefficients

*M.A. Fayazbakhsh, F. Bagheri, M. Bahrami**

Laboratory for Alternative Energy Conversion, School of Mechatronic Systems Engineering, Simon Fraser University, 250-13450 102 Avenue, Surrey, BC, V3T 0A3, Canada

ARTICLE INFO

Article history:
Received 23 January 2015
Received in revised form
30 May 2015
Accepted 30 May 2015
Available online 9 June 2015

Keywords:
HVAC-R
Thermal load calculation
Convection coefficient
Self-adjusting method
Heat balance method

ABSTRACT

A significant step in the design of Heating, Ventilating, Air Conditioning, and Refrigeration (HVAC-R) systems is to calculate the room thermal loads which often vary dynamically. A self-adjusting method is proposed for real-time calculation of heating/cooling loads in HVAC-R applications. In this method, the heat balance calculations are improved by real-time temperature data to achieve more accurate load estimations. An iterative mathematical algorithm is developed to adjust the heat transfer coefficients according to live measurements.

Accepted analytical correlations are also used to estimate the heat transfer coefficients for comparison with the present model. The adjusted coefficients and the analytical correlations are separately used to estimate the thermal loads in an experimental setup. It is shown that the utilization of the adjusted coefficients yields to higher accuracy of thermal load estimations compared to the conventional analytical correlations. Since the proposed method requires less engineering information of the room, it can be adopted as a simplified yet accurate method for the design and retrofit of new and existing HVAC-R systems.

Calcul de charge thermique en temps réel par une estimation automatique des coefficients de convection

Mots clés : CVC-R ; Calcul de charge thermique ; Coefficient de convection ; Méthode d'auto-réglage ; Méthode du bilan thermique

1. Introduction

Heating, Ventilating, Air Conditioning, and Refrigeration (HVAC-R) consume a remarkable portion of the worldwide energy. Half of the total energy usage in buildings as well as 20% of the total national energy usage in European and American countries is consumed by HVAC-R systems (Pérez-Lombard et al., 2008). HVAC-R energy can even exceed half of the total energy usage of a building located in tropical

* *Corresponding author*. Tel.: +1 778 782 8538; fax: +1 778 782 7514.
E-mail address: mbahrami@sfu.ca (M. Bahrami).
http://dx.doi.org/10.1016/j.ijrefrig.2015.05.017
0140-7007/

Nomenclature

a	Sigmoid function parameter
$A[m^2]$	Wall surface area
$c_p[J\ kg^{-1}\ K^{-1}]$	Air specific heat
$c_1, c_2[°C]$	Correlation coefficients
$c_3[s^{-1}]$	Correlation coefficient
C	Correlation coefficient
D	Desired neuron output
f	Sigmoid function
$g[m\ s^{-2}]$	Gravitational constant
$h[W\ m^{-2}\ K^{-1}]$	Convection coefficient
$H[m]$	Wall height
$k[W\ m^{-1}\ K^{-1}]$	Air thermal conductivity
n	Number of walls
O	Calculated neuron output
$P[m]$	Surface perimeter
$\dot{q}[W]$	Heat transfer rate across one wall
$\dot{Q}[W]$	Heat transfer rate
R^2	Coefficient of determination
$t[s]$	Time
$T[°C]$	Temperature
$w_0[W]$	Bias weight factor
$w_j[W\ K^{-1}]$	Input weight factors ($j = 1, \ldots, n$)
$x, y, z[cm]$	Coordinates

Greek letters

$\beta[K^{-1}]$	Volumetric coefficient of thermal expansion
ε	Convergence criterion threshold
η	Learning rate
$\mu[N\ s\ m^{-2}]$	Air dynamic viscosity
$\rho[kg\ m^{-3}]$	Air density

Subscripts and superscripts

a	Air
I	Internal sources
j	Wall number
m	Training step number
V	Ventilation and infiltration
w	Wall surface
W	Walls

climates (Chua et al., 2013). Refrigeration systems also consume a substantial amount of energy. They may use 80% of the total energy in supermarkets (Hovgaard et al., 2011). Moreover, air conditioning is a significant energy-consuming unit in vehicles (Farrington et al., 1999). The air conditioning energy in vehicles outweighs the energy loss to aerodynamic drag, rolling resistance, and driveline losses for a typical vehicle. Air conditioning can reduce the fuel economy of mid-size vehicles by more than 20%. It can also increase vehicle NOx and CO emissions by approximately 80% and 70%, respectively (Farrington and Rugh, 2000). Air conditioning systems of light-duty vehicles consume 7 billion gallons of fuel per year in the United States (Johnson, 2002). Improved design and performance of HVAC-R systems can lead to considerable reductions in the associated energy consumption and gas emissions worldwide.

Thermal load calculation is the primary step in HVAC-R design. It often involves the study of the room characteristics such as wall properties, fenestration, openings, and air distribution. Occupancy level, geographical location, and ambient weather conditions are other necessary data that need to be investigated for thermal load calculations. Considerable engineering effort and time are required for collecting these data. Such detailed information is prone to inaccuracy and may even be unavailable. Therefore, it is promising to develop innovative methods for estimating the thermal loads accurately and with minimum data requirement.

The heat balance method is an effective thermal load calculation technique recognized by the American Society of Heating, Refrigerating and Air-Conditioning Engineers (ASHRAE). The heat balance method is based on the fundamentals of heat transfer and energy balance (ASHRAE, 2009). It is a well-recognized method widely used for calculations in both residential and non-residential applications (Pedersen et al., 1997; Fayazbakhsh and Bahrami, 2013). According to this method, the temperature variation inside a room is the result of the heat transfer through various mechanisms including radiation, convection, and conduction. Among these mechanisms, convection heat transfer has a sophisticated nature and its calculation tends to be complicated and inaccurate.

The convection heat transfer over a wall depends on the velocity and temperature of the air as well as the surface temperature. A common practice for the calculation of the convection heat transfer is to evaluate the coefficients using analytical correlations. ASHRAE Standard 90.1 (ASHRAE, 2013) offers comprehensive tables for the estimation of U-Factors. The U-Factor, or thermal transmittance, is defined as the "heat transmission in unit time through unit area of a material or construction and the boundary air films, induced by unit temperature difference between the environments on each side" (ASHRAE, 2013). However, finding the proper U-Factor requires extensive information to be gathered by the designer. Moreover, the estimated U-Factor may be inaccurate for varying air patterns and thermal conditions.

Besides ASHRAE, other attempts are made to provide reliable estimations of the convection coefficient. A broad range of experimental, computational, and analytical methods is utilized in the literature for estimation of the coefficients. Loveday and Taki (1996) used an experimental arrangement to find correlations for the external convection coefficient as a function of wind speed for a building wall. Kurazumi et al. (2014) experimentally found the convection heat transfer coefficients of human seated body during forced convection by downward flow from the ceiling using a thermal mannequin. Lei et al. (2014) presented an inverse modeling strategy to determine the required wall boundary convection heat fluxes required in computational simulations. In several studies by Zhai et al. (2001), Zhai and Chen (2003b), Zhai and (Yan) Chen (2004), Zhai and Chen (2005), Khalifa (2001a,b), Zhai et al. (2002), Zhai and Chen (2003a), they developed a methodology to couple Computational Fluid Dynamics (CFD) simulations

with Energy Simulations (ES) to improve the accuracy of the latter for different air distribution patterns. They concluded that an ES module coupled with a CFD simulation can benefit from more accurate convection coefficients, hence improving the overall load calculation process (Zhai and Chen, 2003b). However, Zhai and Chen (2005) reported that one CFD calculation may take about 10 h to obtain a reasonable result even with the steady-state condition. Thus, the high time consumption associated to CFD tools is a drawback that hinders their usage in many typical applications.

The amount of studies devoted to the convection coefficient is a notion of its importance. Many reviews have attempted to outline the numerous formulas of convection coefficient. Khalifa (2001a,b) thoroughly reviewed available correlations for natural convection coefficient over flat surfaces. Sartori (2006) reviewed the equations of forced convection coefficient for flow over flat surfaces. Palyvos (2008) presented a survey of the correlations for wind convection coefficient to be used for energy modeling in building envelopes. Defraeye et al. (2011) also collected the existing correlations of convection coefficient over exterior building surfaces and compared them with CFD simulations. From the above reviews, it is evident that the convection coefficient can deeply affect heat balance calculations and an ultimate form that covers all conditions and scenarios is not available. Different values of convection coefficient, even varying by an order of magnitude, can be found in the literature for the same problem. Therefore, an intelligent approach for real-time estimation of the convection coefficient can improve the heat balance calculations significantly.

Conventional methods aim to estimate the convection coefficients according to available correlations and simulations. In such methods, the coefficients are calculated using geometrical and thermal data required in the correlations. However, with the availability of on-site sensors and computational resources, new methodologies focus on the incorporation of real-time data in the calculation process. These are 'data-driven' methods compared to the more conventional 'law-driven' approaches such as the heat balance method.

Data-driven algorithms are proven to be capable of mathematically evaluating thermal loads through measurement and learning rather than mere heat transfer analysis. Several studies (Li et al., Jan. 2009; Kashiwagi and Tobi, 1993; Ben-Nakhi and Mahmoud, 2004; Sousa et al., 1997; Yao et al., 2004; Solmaz et al., 2014; Fayazbakhsh et al., 2015; Wang and Xu, 2006; Wang and Xu, 2006; Liang and Du, 2005) show that artificial intelligence algorithms such as neural networks, genetic algorithm, and fuzzy logic can help estimate the thermal loads in HVAC-R systems. Such models focus on relating the thermal load to parameters such as the ambient temperature by learning from real-time measurements rather than explicitly using the heat transfer equations. However, methods that are purely based on artificial intelligence may be inherently unaware of the heat transfer mechanisms. Therefore, they might be unreliable in new scenarios and conditions for which they are not prepared. The mathematical complexity of some artificial intelligence algorithms may also necessitate large on-site computational resources.

In this study, the heat balance method is combined with a data-driven approach to propose a new algorithm for thermal load calculation. Real-time measurements are used to inversely calculate the convection coefficients, so that those values are further used in the heat balance equation. The model is simple and computationally inexpensive, since it only requires a few algebraic calculations. It is validated using an experimental setup and can aid the design process of new systems and the retrofit of existing systems. HVAC-R controllers can use the real-time load estimations of this method to improve the overall performance of heating/cooling systems. The method is applicable to a wide range of applications including residential buildings, office buildings, freezer rooms, and vehicle air conditioning systems. In the following section, a description of the model is provided, followed by validation and results.

2. Model development

The heat balance equation is considered here as the basis for developing the proposed algorithm. Fig. 1 summarizes the heat balance method as described in the ASHRAE Handbook of Fundamentals (ASHRAE, 2009). As determined at the bottom of Fig. 1, for a heating application at the steady-state condition, *i.e.*, when the heat transfer rates are constant, the heat balance equation is:

$$\dot{Q}_I = \dot{Q}_V + \dot{Q}_W \tag{1}$$

where $\dot{Q}_V$ is the rate of ventilation and infiltration heat loss, $\dot{Q}_W$ is the rate of total heat loss across the walls, and $\dot{Q}_I$ is the heat gain from internal sources. Equation (1) is a balance of thermal energy for the room envelope surrounded by internal wall surfaces.

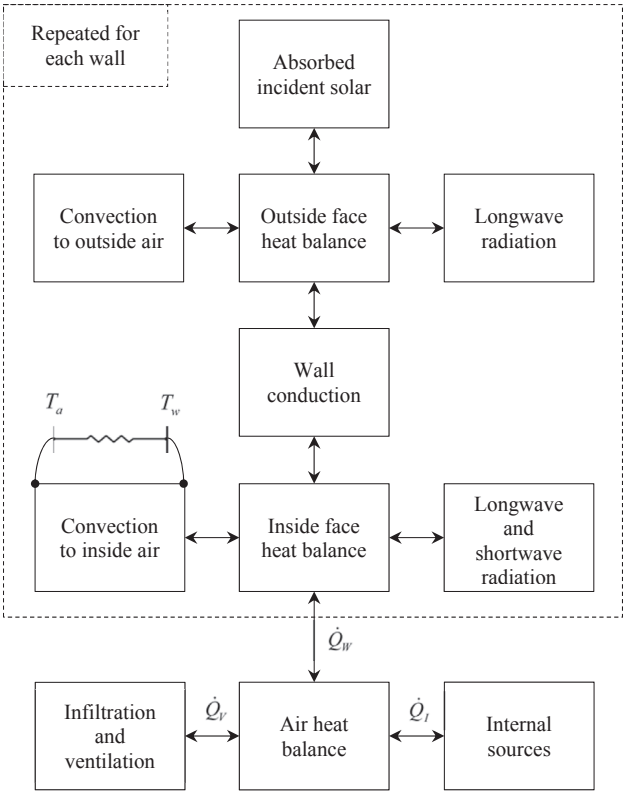

Fig. 1 – Schematic of the heat balance method (ASHRAE, 2009).

Thermal energy is transferred to the wall surfaces by the convection and radiation mechanisms. The convection mechanism depends on various factors such as wall orientation, air velocity, and air temperature. Finding the proper convection coefficients requires correlations that may not hold for all conditions experienced by the room, especially in vehicle applications. Therefore, it is useful to find an estimation of the convection coefficients without excessive experiments or computation.

The other mechanism for transferring heat to the wall surfaces is radiation. A portion of the incident radiation is absorbed by the surfaces and the rest is either reflected or transmitted through. Radiation does not directly increase the air temperature; it transfers energy to the room surfaces, which is in turn transferred to the air through convection and conduction. The bulk of the radiation energy received at each surface contributes to the temperature increase on that surface. Therefore, by directly measuring the surface temperature, the radiation heat transfer is automatically considered in the model.

The calculation of $\dot{Q}_W$ consists of 3 steps: (1) outside face heat balance, (2) conduction through the wall, and (3) inside face heat balance. The total wall heat transfer rate $\dot{Q}_W$ is the summation of all individual wall heat transfer rates $\dot{q}_w$:

$$\dot{Q}_W = \sum_{Walls} \dot{q}_w \tag{2}$$

where $\dot{q}_w$ is the heat transfer rate across each wall. The heat transfer rate is a function of the temperature difference between the wall surface and the adjacent air. Therefore, the inside face heat balance equation can be written as:

$$\dot{q}_w = hA(T_a - T_w) \tag{3}$$

where h is the convection coefficient over the internal surface, A is the wall surface area, T_a is the air temperature adjacent to the wall, and T_w is the temperature on the wall interior surface. In Eq. (3), it is assumed that the wall temperature and air temperature are uniform. Combining Eqs. (2) and (3), the total wall heat transfer rate is written as:

$$\dot{Q}_W = \sum_{j=1}^{n} h_j A_j (T_a - T_w)_j \tag{4}$$

where n is the number of walls.

The heat transfer rate $\dot{Q}_V$ is the result of both the ventilation and infiltration of air. Air may infiltrate into the room through windows and openings and there is often no means of direct measurement to find the volumetric rate of infiltrated air. As such, the accurate rate of heat transfer due to infiltration and ventilation is also unknown in typical applications. Thus, we assume a constant value for the unknown ventilation heat gain, and define it as one of the parameters to be calculated by the algorithm. Replacing $w_0 = \dot{Q}_V$ and $w_j = h_j A_j$ in Eqs. (1) and (4), we arrive at:

$$\dot{Q}_V + \dot{Q}_W = w_0 + \sum_{j=1}^{n} w_j (T_a - T_w)_j \tag{5}$$

The right hand side of Eq. (5) is similar to the linear function of a neuron in neural networks, where w_0 is called the "bias weight" and w_1 to w_n are called the "input weights" (Defraeye et al., 2011; Li et al., 2009; Kashiwagi and Tobi, 1993; Ben-Nakhi and Mahmoud, 2004). Following the common practice in neural networks, we apply a "transfer function" f to the neuron output, defining:

$$O = f\left(w_0 + \sum_{j=1}^{n} w_j (T_a - T_w)_j\right) \tag{6}$$

where O is the neuron output and f is the sigmoid function (Mehrotra et al., 1997) with the following general form:

$$f(a) = \frac{1}{1 + \exp(-a)} \tag{7}$$

In Eq. (7), "a" is a generic parameter used to show the form of the Sigmoid function used in this work.

Eq. (6) is a reformulation of Eq. (1) which is the basic heat balance equation. The convection coefficients which are included in the weight factors "w" in Eq. (6) are still unknown. However, the temperatures T_a and T_w can be measured in real-time. Therefore, an iterative process is proposed to guess and correct the weight factors using the real-time temperature measurements. Since actual measurements are used to update the weight factors, the iterative calculations are called the "training" process.

The last part of the calculations is to update the weight factors according to the current and desired neuron outputs. The original convergence procedure for adjusting the weights was developed by Rosenblatt (1962). Graupe (1997) proved that the weights can be adjusted according to:

$$w_j^{m+1} = w_j^m + \eta (D - O)^m (T_a - T_w)_j^m \tag{8}$$

where m denotes the step number. η is an arbitrary constant called the "learning rate", as it dictates the rate of correction for the weight factors (Lippmann, 1988). Higher learning rates result in faster adjustment of w_j during the training process. However, large η may also cause the weights to diverge to infinity after a few steps. The value of η is often selected by experience. It is assumed that $\eta = 0.05$ throughout this study.

The training procedure is repeated until the convergence criterion is met. Convergence is achieved when all the weights almost remain constant, *i.e.*, their relative variation between two consecutive training steps is less than a certain threshold ε. In this study, a convergence threshold of $\varepsilon = 0.01$ is used.

Once the weights have converged, the training process stops and the weights can be used for the rest of the system's operation, *i.e.*, for other situations when the actual heat gain $\dot{Q}_I$ is unknown. T_a and T_w are measured on all walls and the converged w_j are plugged in Eq. (5) to calculate the total thermal load $\dot{Q}_V + \dot{Q}_w$.

Fig. 2 is a flowchart summarizing the proposed algorithm for thermal load calculation. At the first step, the weight factors should be initiated. If prior estimations are available for h and A from measurements and correlations, the weight factors can be initiated from $w_j = h_j A_j$. However, they can also be initiated from $w_j = 0$, and the iterative process adjusts them until convergence is achieved.

After the weights are initiated the training iterations begin. At every training step, the air temperature (T_a), the surface temperature (T_w), and the internal heat gain ($\dot{Q}_I$) are

measured. In order to measure $\dot{Q}_I$, a known amount of thermal energy can be intentionally introduced into the room. An electrical heater with controllable power consumption can be used to implement the condition. According to Eq. (1), the total heat loss by ventilation, infiltration, and walls is equal to the produced internal heat gain at the steady state. The next step is to calculate the desired neuron output $D = f(\dot{Q}_I)$ and the current neuron output O from Eq. (6). The Sigmoid function defined in Eq. (7) is used for calculating the parameters D and O.

The results of the proposed model greatly rely on the temperature measurements. It is necessary to have at least one thermocouple pair on each wall. The temperature, geometry, and convection coefficient are assumed uniform in the model. These assumptions may be inaccurate for large walls and complicated rooms. Additional thermocouple pairs can obviously improve the model accuracy, especially in large rooms. It is recommended to virtually divide the walls into various sectors and attribute an independent temperature value to each sector. Therefore, the accuracy of the resulting convection coefficients can improve in the same way as finer meshes would improve the computational simulations of the room heat transfer. As the measuring technologies improve and new facilities become available, the model can be extended and verified in more complicated geometries and larger rooms.

The model is validated for a heating scenario and the results are presented in the following section. Since the general heat balance equation is used for developing the model, it can be readily extended to cooling scenarios and different room dimensions.

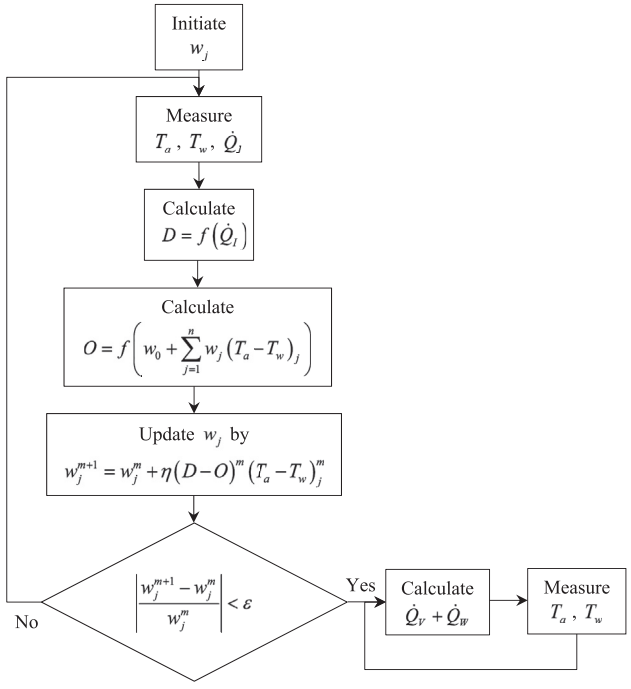

Fig. 2 – Flowchart of the algorithm for real-time thermal load calculation by automatic estimation of convection coefficients.

3. Results and discussion

A testbed is built to test and verify the proposed model. Fig. 3 shows the testbed built out of wood, plastic, and glass. It is designed as a generic chamber in which heating and air conditioning scenarios can be tested. Six pairs of T-type thermocouples (5SRTC-TT-T-30-36, Omega Engineering Inc., Laval, QC, Canada) are attached on its walls. Out of every pair, one thermocouple is attached to the interior wall surface and the other is hung in the interior air adjacent to the same spot. The air-side thermocouple is located at an approximate distance of 1 cm apart from the wall.

Heat convection heavily depends on both the surface geometry and the local flow characteristics. For instance, the reading of a thermocouple pair located close to a wall edge is not identical to one installed on a wide open wall center. There is always conjugate (conduction and convection) heat transfer taking place at surface edges and the effect is more significant when non-conductive materials are involved. Thus, attributing a single convection coefficient to an entire wall is an approximate yet accepted approach. Although temperature readings are performed at individual spots, the

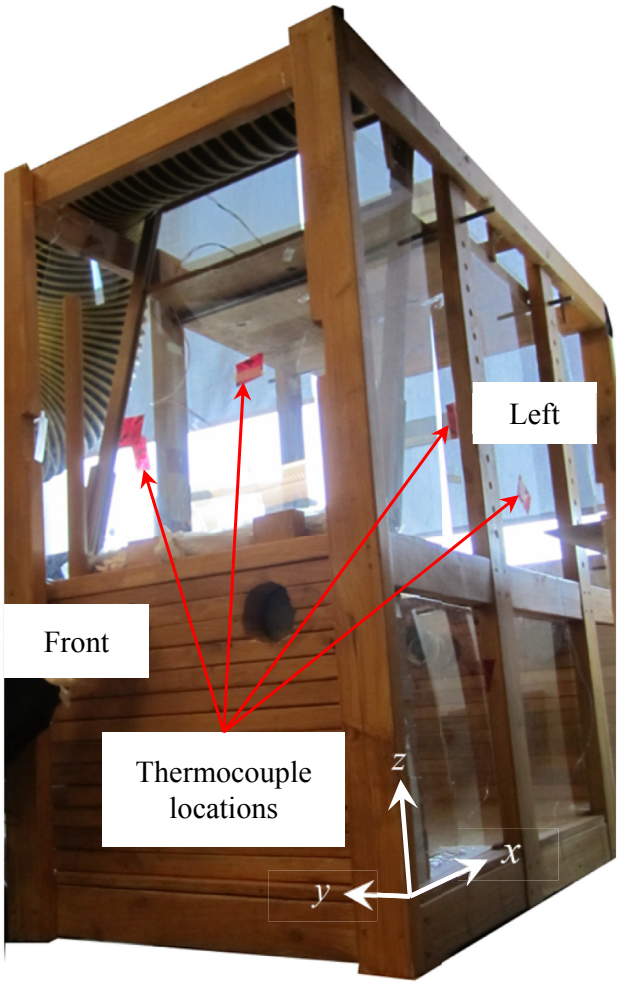

Fig. 3 – The testbed used for model validation. Six thermocouple pairs are attached to the walls by tape.

Table 1 – Location of thermocouples with reference to the coordinate system shown in Fig. 3.

Thermocouple Pair name	x(cm)	y(cm)	z(cm)
Front	10	38	139
Rear	147	38	148
Left	80	0	85
Right	35	75	100
Top	55	55	131
Bottom	55	65	0

proposed model also follows the same accepted approach and assumes a single convection coefficient (weight factor) for each wall.

More thermocouple pairs can definitely increase the accuracy of thermal load calculations. However, the locations of the limited number of thermocouple pairs used in this testbed are arbitrarily selected and, in turn, the self-adjusting algorithm attempts to iteratively adjust the coefficients using the local temperature readings. Unless rigorous three-dimensional CFD simulations or extensive experiments are performed, the detailed heat convection from the surface is unknown. Thus, the weight factors w_j calculated for every thermocouple pair are assumed as the average coefficient $h_j A_j$ at the corresponding wall.

The thermocouples have a tolerance of ±1.0°C and are connected to a data acquisition system (NI 9214DAQ, National Instruments Canada, Vaudreuil-Dorion, QC, Canada) that logs the temperatures at a frequency of 1 Hz. Before starting the experiments, the thermocouples are tested for calibration at the room temperature without any heating or cooling. The thermocouple pairs show the same temperature at every location with a maximum error of ±0.1°C. Since only temperature differences are used in the model, the relative calibration of thermocouple pairs proves that the tolerances of ±1°C are compensated and the errors are cancelled by the subtraction $(T_a - T_w)$. Therefore, the temperature difference values can be reliably used for the heat transfer calculations of the present model.

Regular tape is used to attach the thermocouples as seen in Fig. 3. The four openings on the front and rear walls of the chamber are blocked and the chamber is sealed in order to avoid air infiltration and ventilation. However, a small amount of infiltration may still exist due to imperfect air sealing.

Table 1 shows the thermocouple locations with reference to the coordinate system shown in Fig. 3. As described above, the thermocouple locations are arbitrarily selected. These locations are intentionally not symmetric, so that the generality of the self-adjusting technique for arbitrary configurations is showcased. Fig. 4 shows a computer model of the chamber alongside its cross section in a cut view. Overall chamber dimensions are also shown in Fig. 4 and the names of different components are indicated.

An electrical heater with controlled power input is placed inside the chamber on the bottom plate. The heater is equipped with a fan to circulate air inside the chamber. The fan is kept at the same location for all tests. The fan power is measured as 10 W and is eventually converted to heat in the enclosed chamber due to damping of the air motion. Therefore, the fan power is also added to the total heating power in all calculations.

The heater consists of a resistor that provides Joule heating with controlled input power. The amount of power provided to the heater is controlled and monitored by a programmable DC power supply (62000P, Chroma Systems Solutions Inc., Orange County, CA, US). The maximum error of the power measurements is ±0.1 W. Since there is no other heat source available in the chamber, the known power input to the fan

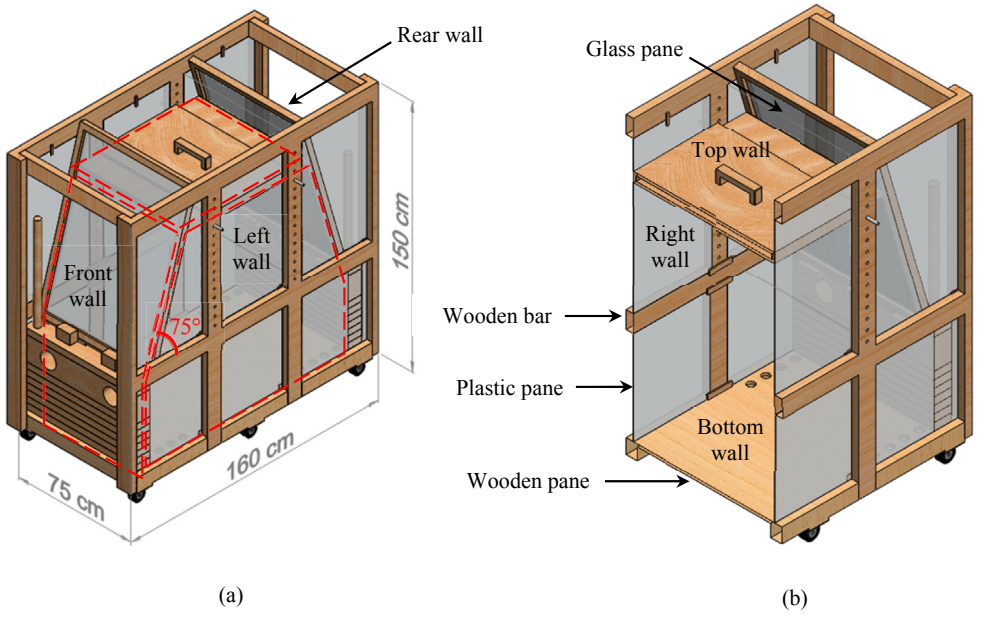

Fig. 4 – Computer model of the testbed showing its overall dimensions and components. (a) Full view. (b) Cross sectional view.

and heater can be assumed as the direct heat gain from internal sources $\dot{Q}_I$.

An experiment is conducted on the testbed for validating the proposed model. Various amounts of direct internal heat gain are imposed on the chamber by varying the DC power provided to the heater. The heater power is kept constant at each level until it is ensured that the steady-state condition is reached. The measurements are recorded for analysis and calculation.

ASHRAE Handbook of Fundamentals (ASHRAE, 2009) provides analytical correlations for finding the natural convection coefficients over vertical and horizontal surfaces. Following the conventional method of thermal load calculation, these coefficients can be used for estimating the heat transfer across the walls. To validate the present model, the analytical correlations are applied on the testbed and the resulting convection coefficients are compared to the calculated weight factors. Moreover, the total thermal load is calculated using both sets of coefficients to showcase the effectiveness of the proposed model. Eq. (4) is used to calculate the heat gain by the analytical formulas of convection coefficient. Similarly, Eq. (5) is used to calculate the thermal load by the weight factors of the present model.

The analytical coefficient of air natural convection over a vertical wall is calculated from (ASHRAE, 2009):

$$h = 1.33\left(\frac{T_a - T_w}{H}\right)^{1/4} \tag{9}$$

where H is the wall height. The coefficient of air natural convection over a horizontal surface is calculated from (ASHRAE, 2009):

$$h = C\left(\frac{g\beta\rho^2 k^3 c_p P}{\mu A}(T_a - T_w)\right)^{1/4} \tag{10}$$

where g is the gravitational constant, β is the volumetric coefficient of thermal expansion, ρ is the air density, k is the air thermal conductivity, c_p is the air specific heat, P is the wall perimeter, and μ is the air dynamic viscosity. $C = 0.54$ for a cold surface facing down and $C = 0.27$ for a cold surface facing up. Table 2 shows the estimated convection coefficients according to Eqs. (9) and (10), where the average measured temperatures during the validation experiment are used for T_a and T_w.

Eq. (1) which is the basis of the present model assumes the steady-state condition. Therefore, it is required to ensure that the steady-state condition is reached for every level of the heater power in the validation experiment. The steady-state values of the heat transfer rates $\dot{Q}$ are reached when all temperature differences $T_a - T_w$ reach relatively constant levels. Thus, the exponential growth of the temperature differences from the initial values are observed and exponential correlations of the form:

$$T_a - T_w = c_1 + c_2 \exp(-c_3 t) \tag{11}$$

are applied on them. c_2 is negative for the increasing exponential trends. The correlation of Eq. (11) is applied to the measurements from all thermocouple pairs with minimum coefficients of determination calculated as $R^2 = 0.95$. Fig. 5 shows the exponential growth of the temperature difference $T_a - T_w$ on the left wall from an initial steady-state. The exponential correlation fitted over the temperature scatters has a time constant of 226 s, *i.e.*, it takes less than 4 min for the temperature difference to reach 99% of its maximum steady-state value. The same procedure is applied to all walls and the maximum time constant is calculated as 335 s on all walls. Hence, to ensure that the steady condition is reached, the heater power is kept constant for 10 min at every level and the final measurements are used in the calculation of thermal loads.

As shown in Fig. 2, the first part of the algorithm consists of training the weight factors through an experiment where the direct heat gain $\dot{Q}_I$ is known. In order to find the adjusted coefficients, the testbed is allowed to reach the steady state at an arbitrary level $\dot{Q}_I = 0.334$ kW of the heater power. Then, the training algorithm is run until the convergence criteria:

$$\left|\frac{w_j^{m+1} - w_j^m}{w_j^m}\right| < \varepsilon \tag{12}$$

is met with $\varepsilon = 0.01$. At every step, the weight factors are corrected according to Eq. (8). Fig. 6 shows the progressive adjustment of the weight factors during the training process.

Table 2 – Wall surface areas and convection coefficients calculated from analytical correlations (ASHRAE, 2009) shown in Eqs. (9) and (10). Refer to Fig. 4 for component names and locations.

Wall name	A (m^2)	h (W m^{-2} K^{-1})	hA (W K^{-1})
Front	0.5	1.73	0.85
Rear	0.5	1.61	0.78
Left	2.0	1.76	3.42
Right	2.0	1.59	3.09
Top	2.0	1.61	3.23
Bottom	3.0	0.86	2.58

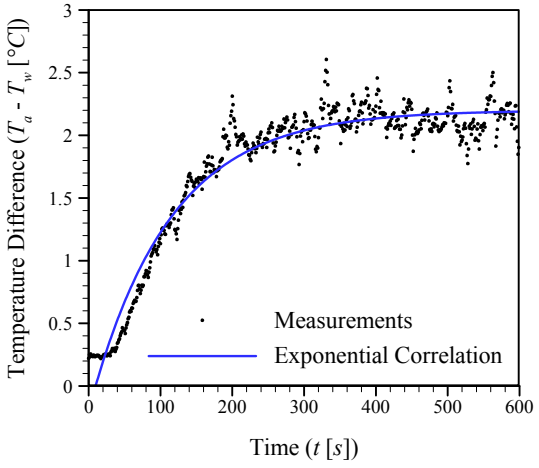

Fig. 5 – Exponential growth of the temperature difference ($T_a - T_w$) to the steady-state condition on the left wall. The exponential correlation of Eq. (11) is fitted on the measurements.

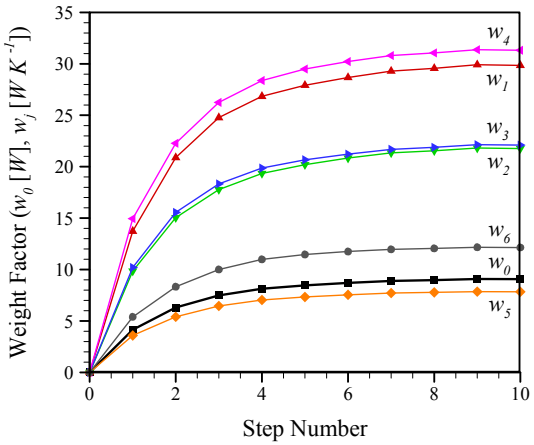

Fig. 6 – Progressive adjustment (training) of the weight factors at an arbitrary heater power of $\dot{Q}_I = 0.334$ kW.

All the weight factors are initiated at zero, and the convergence is achieved within 10 steps.

Fig. 7 shows the convergence of the calculated heat gain to the measured value during the training process. As the weight factors are updated, the calculation of the heat gain $\dot{Q}_I$ becomes more accurate step by step until convergence to the measured value is achieved.

Table 3 shows the converged values of the weight factors shown in Fig. 6. The coefficients hA from Table 2 for each wall are also repeated in Table 3 for comparison. Since $\dot{Q}_V$ is unknown, the converged value of its mathematical equivalent w_0 is used for the ventilation term when calculating the total heat gain from analytical correlations. It is noted that the coefficients hA (calculated from analytical correlations) and their mathematical equivalents w_j (adjusted by the training algorithm) can have remarkably different values. In this case, the available analytical correlations largely underestimate the rate of heat transfer across the walls. Therefore, automatic adjustment of coefficients can be beneficial for more accurate estimation of thermal loads.

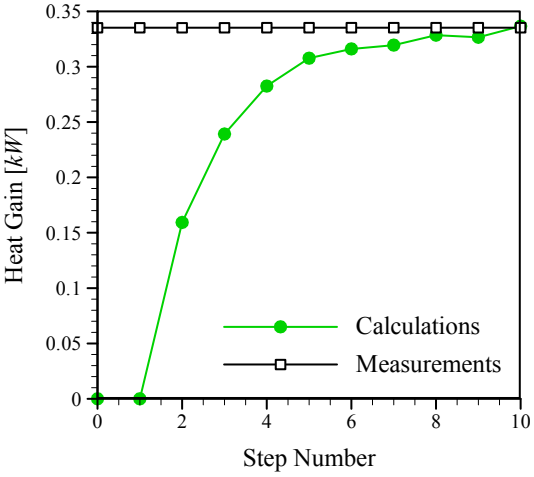

Fig. 7 – Progressive correction of the calculated heat gain during the training process at a measured heat gain of $\dot{Q}_I = 0.334$ kW.

Table 3 – Comparison of adjusted weight factors with convection coefficients from analytical formulas.

Convection coefficient	Analytical Value	Adjusted Value
Ventilation and infiltration	$\dot{Q}_V = 9.11$ W[a]	$w_0 = 9.11$ W
Front Wall	$h_1A_1 = 0.85$ W K^{-1}	$w_1 = 29.4$ W K^{-1}
Rear Wall	$h_2A_2 = 0.78$ W K^{-1}	$w_2 = 21.1$ W K^{-1}
Left Wall	$h_3A_3 = 3.42$ W K^{-1}	$w_3 = 21.8$ W K^{-1}
Right Wall	$h_4A_4 = 3.09$ W K^{-1}	$w_4 = 31.4$ W K^{-1}
Top Wall	$h_5A_5 = 3.23$ W K^{-1}	$w_5 = 7.82$ W K^{-1}
Bottom Wall	$h_6A_6 = 2.58$ W K^{-1}	$w_6 = 12.0$ W K^{-1}

[a] Estimated equal to w_0.

The convection coefficients from analytical correlations and those adjusted by the training algorithm of the present model are used to calculate the total heat gain. Fig. 8 shows the results using both sets of coefficients at various levels of steady-state heater power. It is noted that analytical coefficients can result in huge errors for the calculation of the total heat gain. In this specific case, there is a minimum of 67% error in the heat gain calculation using analytical coefficients. The adjusted weight factors, however, result in a maximum error of 9%.

The analytical correlations are rigorously validated by analysis and experiment. But they contain certain assumptions that confine their usage. For instance, they assume natural convection over a flat wall and provide the average convection coefficient over the wall in its wide open area. They also assume uniform wall temperature. In practice, none of these assumptions completely hold. In the present experiment, the walls are surrounded by other enclosure walls, they are not completely flat, some forced convection may occur over them, and they have non-uniform temperatures. To find more accurate convection coefficients, detailed experiments or numerical simulations are required. The present algorithm is proposed as a tool for providing accurate thermal load calculations while avoiding extensive simulations and experiments.

As a data-driven method, a disadvantage of the present model is that it requires training. Although the training can be

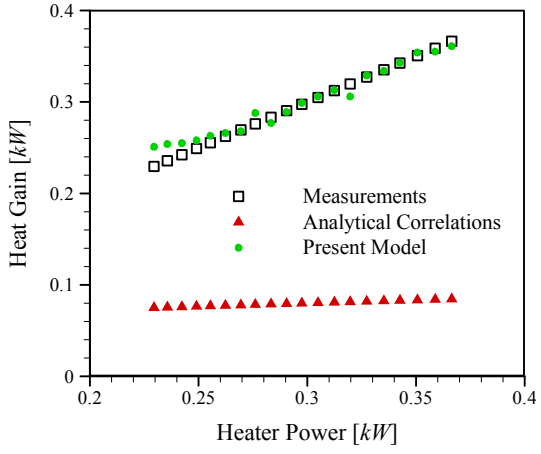

Fig. 8 – Heat gain calculated by the analytical correlations and the adjusted weight factors by the present model.

performed within seconds, directly measuring the heat gain may be impossible in many cases. However, it is possible to artificially impose a known heat gain to an existing room using the same testing approach of this study, *i.e.*, isolating the room from all possible thermal loads except a known source of internal heating or cooling. As such, this method can be used for retrofitting existing systems as well as designing new systems. Whenever it is impossible to directly test the room for the training process, conventional law-driven methods can be used to provide an estimation of the actual heat gain. The estimated heat gain can be fed to the algorithm as the training target for $\dot{Q}_I$. The algorithm can then use the adjusted coefficients for calculating the real-time thermal loads based on future temperature measurements.

4. Conclusions

A method is proposed for real-time calculation of thermal loads in HVAC-R applications by automatic estimation of convection coefficients. The convection coefficients required by the heat balance equation are adjusted using a mathematical algorithm and temperature measurements. The proposed method is validated by experimental results. It is shown in a case study that the algorithm can calculate the heat gain with a maximum error of 9%, whereas unadjusted coefficients calculated from analytical correlations result in a minimum error of 67%. Since the proposed method is based on fundamental heat transfer equations, it can be used in a wide range of stationary and mobile applications. It provides a simple tool for designing new systems and retrofitting existing ones while avoiding extensive simulations and experiments.

Acknowledgments

This work was supported by Automotive Partnership Canada (APC), Grant No. NSERC APCPJ/429698-11. The authors would like to thank the kind support of the Cool-It Group, 100-663 Sumas Way, Abbotsford, BC, Canada. The authors wish to acknowledge David Sticha for his efforts in building the testbed.

REFERENCES

ASHRAE, 2009. Handbook of Fundamentals. American Society of Heating, Refrigerating and Air-Conditioning, Atlanta.
ASHRAE, 2013. Standard 90.1–2013, Energy Standard for Buildings Except Low Rise Residential Buildings. American Society of Heating, Refrigerating and Air Conditioning Engineers.
Ben-Nakhi, A.E., Mahmoud, M.A., Aug. 2004. Cooling load prediction for buildings using general regression neural networks. Energy Convers. Manag. 45 (13–14), 2127–2141.
Chua, K.J., Chou, S.K., Yang, W.M., Yan, J., Apr. 2013. Achieving better energy-efficient air conditioning – a review of technologies and strategies. Appl. Energy 104, 87–104.
Defraeye, T., Blocken, B., Carmeliet, J., 2011. Convective heat transfer coefficients for exterior building surfaces: existing correlations and CFD modelling. Energy Convers. Manag. 32 (0), 1–20.
Farrington, R., Rugh, J., 2000. "Impact of Vehicle Air-conditioning on Fuel Economy, Tailpipe Emissions, and Electric Vehicle Range," in Earth Technologies Forum no. September.
Farrington, R., Cuddy, M., Keyser, M., Rugh, J., 1999. Opportunities to reduce air-conditioning loads through lower cabin soak temperatures. In: Proceedings of the 16th Electric Vehicle Symposium.
Fayazbakhsh, M.A., Bahrami, M., 2013. "Comprehensive Modeling of Vehicle Air Conditioning Loads Using Heat Balance Method," in SAE Transactions.
Fayazbakhsh, M.A., Bagheri, F., Bahrami, M., Jan. 2015. An inverse method for calculation of thermal inertia and heat gain in air conditioning and refrigeration systems. Appl. Energy 138, 496–504.
Graupe, D., 1997. Principles of Artificial Neural Networks.
Hovgaard, T., Larsen, L., Skovrup, M., Jørgensen, J., 2011. Power consumption in refrigeration systems-modeling for optimization. In: Proceedings of the 2011 4th International International Symposium on Advanced Control of Industrial Processes, pp. 234–239.
Johnson, V.H., 2002. Fuel Used for Vehicle Air Conditioning: a State-by-State Thermal Comfort-Based Approach. SAE Transactions.
Kashiwagi, N., Tobi, T., 1993. Heating and cooling load prediction using a neural network system. In: Proceedings of 1993 International Conference on Neural Networks (IJCNN-93-Nagoya, Japan), vol. 1, pp. 939–942.
Khalifa, A., 2001. Natural convective heat transfer coefficient–a review: I. Isolated vertical and horizontal surfaces. Energy Convers. Manag. 42.
Khalifa, A., 2001. Natural convective heat transfer coefficient–a review: II. Surfaces in two-and three-dimensional enclosures. Energy Convers. Manag. 42.
Kurazumi, Y., Rezgals, L., Melikov, A., 2014. Convective heat transfer coefficients of the human body under forced convection from ceiling. J. Ergon. 4 (1), 1–6.
Lei, L., Wang, S., (Tim) Zhang, T., Apr. 2014. Inverse determination of wall boundary convective heat fluxes in indoor environments based on CFD. Energy Build. 73, 130–136.
Li, Q., Meng, Q., Cai, J., Yoshino, H., Mochida, A., Jan. 2009. Predicting hourly cooling load in the building: a comparison of support vector machine and different artificial neural networks. Energy Convers. Manag. 50 (1), 90–96.
Liang, J., Du, R., 2005. Thermal comfort control based on neural network for HVAC application,". In: Proceedings of 2005 IEEE Conference on Control Applications, 2005. CCA 2005, pp. 819–824.
Lippmann, R.P., Mar. 1988. An introduction to computing with neural nets. ACM SIGARCH Comput. Archit. News 16 (1), 7–25.
Loveday, D.L., Taki, A.H., May 1996. Convective heat transfer coefficients at a plane surface on a full-scale building facade. Int. J. Heat Mass Transf. 39 (8), 1729–1742.
Mehrotra, K., Mohan, C., Ranka, S., 1997. Elements of Artificial Neural Networks. MIT Press.
Palyvos, J.A., Jun. 2008. A survey of wind convection coefficient correlations for building envelope energy systems' modeling. Appl. Therm. Eng. 28 (8–9), 801–808.
Pedersen, C.O., Fisher, D.E., Liesen, R.J., 1997. Development of a heat balance procedure for calculating cooling loads. ASHRAE Trans. 103, 459–468.
Pérez-Lombard, L., Ortiz, J., Pout, C., Jan. 2008. A review on buildings energy consumption information. Energy Build. 40 (3), 394–398.
Rosenblatt, F., 1962. Principles of Neurodynamics.
Sartori, E., Sep. 2006. Convection coefficient equations for forced air flow over flat surfaces. Sol. Energy 80 (9), 1063–1071.
Solmaz, O., Ozgoren, M., Aksoy, M.H., Jun. 2014. Hourly cooling load prediction of a vehicle in the southern region of Turkey

by artificial neural network. Energy Convers. Manag. 82, 177–187.
Sousa, J.M., Babuška, R., Verbruggen, H.B., Oct. 1997. Fuzzy predictive control applied to an air-conditioning system. Control Eng. Pract. 5 (10), 1395–1406.
Wang, S., Xu, X., Apr. 2006. Simplified building model for transient thermal performance estimation using GA-based parameter identification. Int. J. Therm. Sci. 45 (4), 419–432.
Wang, S., Xu, X., Aug. 2006. Parameter estimation of internal thermal mass of building dynamic models using genetic algorithm. Energy Convers. Manag. 47 (13–14), 1927–1941.
Yao, Y., Lian, Z., Liu, S., Hou, Z., Nov. 2004. "Hourly cooling load prediction by a combined forecasting model based on analytic hierarchy process. Int. J. Therm. Sci. 43 (11), 1107–1118.
Zhai, Z., Chen, Q., 2003. Impact of determination of convective heat transfer on the coupled energy and CFD simulation for buildings. In: Proceedings of Building Simulation Conference, pp. 1467–1474.
Zhai, Z., Chen, Q., 2003. Solution characters of iterative coupling between energy simulation and CFD programs. Energy Build. 35, 493–505.
Zhai, Z.J., Chen, Q.Y., Apr. 2005. Performance of coupled building energy and CFD simulations. Energy Build. 37 (4), 333–344.
Zhai, Z., (Yan) Chen, Q., Aug. 2004. Numerical determination and treatment of convective heat transfer coefficient in the coupled building energy and CFD simulation. Build. Environ. 39 (8), 1001–1009.
Zhai, Z., Chen, Q., Klems, J.H., Haves, P., 2001. Strategies for Coupling Energy Simulation and Computational Fluid Dynamics Programs.
Zhai, Z., Chen, Q., Haves, P., Klems, J.H., 2002. On approaches to couple energy simulation and computational fluid dynamics programs. Build. Environ. 37, 857–864.